Deterministic phase unwrapping in the presence of noise

Vyacheslav V. Volkov and Yimei Zhu

Department of Materials Science, Brookhaven National Laboratory, Upton, New York 11973-5000

Received March 28, 2003

We present a new Fourier-based exact solution for deterministic phase unwrapping from experimental maps of wrapped phase in the presence of noise and phase vortices. This single-step approach has superior performance for images with high phase gradients or insufficient digital sampling approaching 2π/pixel and therefore performs as a fast and practical solution for the phase-unwrapping problem for experimental applications in applied optics, physics, and medicine.

OCIS codes: 100.5070, 050.5080, 120.5050, 010.1080, 030.6610, 090.2880, 280.6730, 070.2590, 350.5030.

The ability to determine a true phase map from the principal noisy value of a wrapped phase is essential for many fields in applied optics, physics, medicine, and engineering, including geodesic and military applications that deal with coherent wave processes, such as homomorphic signal processing,[1] solid-state physics,[2] speckle interferometry,[3,4] adaptive or compensated optics,[5] magnetic resonance imaging,[6,7] and synthetic aperture radar interferometry.[8] It is also essential in optical and electron holography,[9] since any wrapped phase map is defined by its principal value $0 \leq \varphi_w(\mathbf{r}) < 2\pi$, whereas the spatially varying true phase $\varphi(\mathbf{r})$, which measures real physical quantities (such as thickness or potential map, temperature, or deformation fields), can span many π. Therefore phase unwrapping must be carried out before any reconstruction of the physical quantities from the given phase map. Recovery of the true phase $\varphi(\mathbf{r})$ from the noisy principal value $\varphi_w(\mathbf{r})$, known as the phase-unwrapping process, is described by the following equation, which is valid for all $\mathbf{r} = (x, y, z) \in \Omega$:

$$\varphi_w(\mathbf{r}) + 2\pi k(\mathbf{r}) = \varphi(\mathbf{r}) + n(\mathbf{r}), \tag{1}$$

where $k(\mathbf{r})$ is a solution for the integer number field and transforms Eq. (1) into an identity; $n(\mathbf{r})$ is the experimental noise function. Several algorithms for phase unwrapping in the presence of noise have been reported (see, for example, Refs. 10–12 and references therein), but only a few of them are good enough for practical applications (with limitations such as user input, median filtering, computing time, image size, and absence of phase vortices). The main problem that causes many of these approaches to fail is that they are one dimensional, based on column-by-column (raw-by-raw) operation. To overcome this problem, a path-independent solution of the Poisson equation was suggested in Ref. 13 and in an advanced version in Ref. 14. However, in Refs. 13 and 14 it was necessary to postulate appropriate boundary conditions that did not follow from the experiment. In addition, any use of Laplacian operators on digital data requires kernels of at least 3×3 pixels. Hence this approach may fail in the case of strong phase oscillations or undersampled data.

In this Letter we report a new Fourier-transform-based single-step phase-unwrapping procedure with the minimal theoretically possible kernel size of 2×1 pixels. This procedure is immune to noise, path independent, fast, and robust. It is ideal for phase maps with marginal sampling and is free from the boundary constraints required by the solution of the Poisson equation. Phase unwrapping that is unique to an additive constant is realized by the exact Fourier solution through Eq. (3). For digital phase reconstruction we assume only that local phase and noise-related phase jumps do not exceed 2π/pixel. This makes sense for strongly undersampled objects. Otherwise, the definition of digitized wrapped phase itself is not single valued. In addition, the unwrapping of statistical noise, exceeding 2π/pixel phase jumps (FWHM > 1.57), would change the statistic of the Gaussian noise, and Eq. (1) would not have a unique $k(\mathbf{r})$ solution from a physical point of view.

It is known that any differentiable scalar function $\psi(\mathbf{r})$ can be uniquely recovered up to some constant in a simple bounded area Ω, if the derivatives $\partial_x\psi(\mathbf{r})$ and $\partial_y\psi(\mathbf{r})$ exist everywhere in this area. However, any direct integration of the derivatives for phase unwrapping results in an unreliable path-dependent solution. Unwrapping it is often complicated by the presence of phase vortices and noise, and, in general, it fails (see Fig. 1b). On the other hand, this problem can be solved in Fourier space. First note two remarkable properties that are valid for forward (F) and inverse (F^{-1}) Fourier transforms with $\mathbf{r}$ and $\mathbf{q}$ vectors operating in real and reciprocal space:

$$\nabla[\exp(2\pi i\mathbf{q} \cdot \mathbf{r})] = 2\pi i\mathbf{q}[\exp(2\pi i\mathbf{q} \cdot \mathbf{r})], \tag{2a}$$

$$\nabla\psi(\mathbf{r}) = 2\pi i F^{-1}\{F[\psi(\mathbf{r})]\mathbf{q}\}. \tag{2b}$$

The vector identity in Eq. (2a) is trivial, whereas the second vector identity in Eq. (2b), which is valid for any differentiable scalar complex function $\psi(\mathbf{r})$, can be derived by component analysis with Eq. (2a). Repeated use of this identity as $\nabla(\nabla\psi) = \nabla^2\psi$ helps solve the nonholographic phase retrieval problem as well.[15,16] Next, by applying the F operator to Eq. (2b) and making its scalar products with $\mathbf{q}(q_x, q_y, q_z)$ components, we get a new expression for the scalar real or complex function $\psi(\mathbf{r})$ in two-dimensional space:

$$\psi(\mathbf{r}) = \mathrm{Re}\left\{\frac{1}{2\pi i} F^{-1}\left[\frac{F(\partial_x\psi)q_x + F(\partial_y\psi)q_y}{q_\perp^2}\right]\right\}. \tag{3}$$

Here q_x and q_y are the spatial projections of the wave vector $\mathbf{q}_\perp$ defined by modulus as $q_\perp^2 = q_x^2 + q_y^2 \neq 0$.

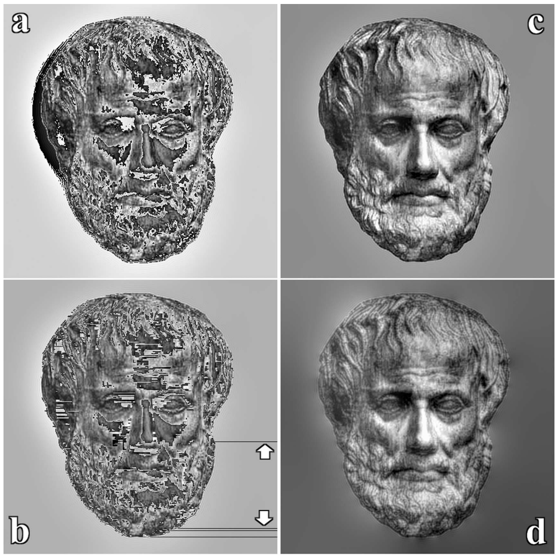

Fig. 1. Image of sculpture of Aristotle, illustrating several aspects of the phase-unwrapping process. (a) Synthetic wrapped phase of 512 × 512 pixels obtained from an image identical to the image shown in (c). (b) Best phase unwrapping by the conventional path-dependent approach, creating artifacts marked by arrows. (c) Exact and (d) approximate solutions with Fourier transform via Eq. (3). Note that the maximal phase variation in (c) is 14.4 rad with local phase gradients as high as 4.07 rad/pixel. The unwrapped phase (c) is pixel to pixel identical to the original image.

The transform via Eq. (3) is unique up to some constant, since the behavior of function $\psi(\mathbf{r})$ is defined by the Neumann boundary condition for its known derivatives. A unique and nonspoiled Fourier solution via Eq. (3) can be obtained by use of the symmetrization rule.[16] Since integration by Eq. (3) is performed in $\mathbf{q}$ space, the solution appears to be path independent and immune to noise and phase vortices in the real-space image.

To recover the phase with Eq. (3), we need to know only the $\partial_x\psi(\mathbf{r})$ and $\partial_y\psi(\mathbf{r})$ components of the gradient function $\nabla_\perp\psi(\mathbf{r})$. Further, for the phase-unwrapping problem we assume that $\psi(\mathbf{r})$ is related to a real noisy function to be retrieved from Eq. (1) as $\psi(\mathbf{r}) = \varphi(\mathbf{r}) + n(\mathbf{r})$, whereas the wrapped phase $\varphi_w(\mathbf{r})$ is generated by the wrapping operator $\varphi_w(\mathbf{r}) = W[\varphi(\mathbf{r}) + n(\mathbf{r})]$. Notice that the x and y derivatives of the real noisy phase and the wrapped phase are identical in $\mathbf{r}$ space, except for a few special single-pixel false lines or pixels where 2π/pixel phase jumps occur because of the digital wrapping for the $\varphi_w(\mathbf{r})$ phase. Hence, with appropriate correction of the false pixels in $\nabla_\perp\varphi_w(\mathbf{r})$ gradient map it becomes possible to equate the x and y components such that $\partial_x\psi(\mathbf{r}) \cong \partial_x\varphi_w(\mathbf{r})$ and $\partial_y\psi(\mathbf{r}) \cong \partial_y\varphi_w(\mathbf{r})$ and to recover a phase $\psi(\mathbf{r})$ through Eq. (3). We recommend this effective, robust solution for Eq. (1) that always exists for any on-line phase-unwrapping procedure no matter how complex the phase wrap. However, we shall call it an approximate solution, because for digital image processing it may not provide perfect correction of false pixels (typical error of <2%) in local areas with phase jumps approaching 2π/pixel (illustrated in Fig. 1d). Therefore for ideal phase unwrapping (an exact solution) it is better to recover the $2\pi k(\mathbf{r})$ function with the $k(\mathbf{r})$ integer field with the experimental $\varphi_w(\mathbf{r})$ function remaining untouched. Indeed, by taking the gradient of Eq. (1), we find $2\pi\nabla_\perp k(\mathbf{r}) = \nabla_\perp\psi(\mathbf{r}) - \nabla_\perp\varphi_w(\mathbf{r})$, where the only unknown function, $\nabla_\perp\psi(\mathbf{r})$, can be found from Eq. (1) and rewritten as

$$Z(\mathbf{r}) = \exp\{i[\varphi_w(\mathbf{r}) + 2\pi k(\mathbf{r})]\} = \exp[i\varphi_w(\mathbf{r})]. \quad (4)$$

There exists a useful relation $\nabla_\perp\psi(\mathbf{r}) = \mathrm{Re}[\nabla_\perp Z(\mathbf{r})/iZ(\mathbf{r})]$ with well-defined complex function $Z(\mathbf{r}) = \exp[i\varphi_w(\mathbf{r})]$ free from 2π jumps generated by the phase-wrapping operator. Actually, this is a simple means of constructing the $\nabla_\perp\psi(\mathbf{r})$ gradient map required by the approximate solution. For the exact solution, constrained only by finite image sampling, our false lines or pixels, generated by the wrapping operator, are described by the vector relation $2\pi\nabla_\perp k(\mathbf{r}) = \mathrm{Re}[\nabla_\perp Z(\mathbf{r})/iZ(\mathbf{r})] - \nabla_\perp\varphi_w(\mathbf{r})$. Hence, by substituting the known components $\partial_x k(\mathbf{r})$ and $\partial_y k(\mathbf{r})$ into Eq. (3) through Eq. (4), we recover in a single step the whole field of integer numbers $k(\mathbf{r})$ and make Eq. (1) an identity. This exact solution (see Fig. 1c) forms the basis for deterministic phase unwrapping with a Fourier transform through Eq. (3).

To demonstrate the power of this new approach, we consider three very different examples of the phase-unwrapping process, which highlight several aspects of this problem. The first example of a phase map, modeled in Fig. 1, is characterized by phase gradients as high as $2\pi/1.5$ pixel. Although the traditional path-dependent approach (Fig. 1b) fails to unwrap the phase $\varphi_w(\mathbf{r})$ (Fig. 1a), both the exact (Fig. 1c) and the approximate (Fig. 1d) solutions reproduce the original phase image identical to the solution in Fig. 1c. As mentioned above, the single-step approximate solution serves as a perfect guide for any complex phase unwrapping, because it always exists, whereas the exact solution may not be obtained in practice, for instance, because of insufficient digital sampling with gradients greater than 2π/pixel.

Another example of noisy phase retrieval in the presence of rapid phase variations, vortices, and noise is shown in Fig. 2. The wrapped phase (Fig. 2a) contains Gaussian noise with phase jumps as high as 1.95π/pixel. The exact phase solution from Eq. (3) is shown in Fig. 2b. It fits pixel to pixel with the original image used to model the crystal lattice potential. Note that retrieval of a phase map that is 512 × 512 pixels usually takes a few seconds on a Dell (500 MHz) personal computer. Our method is also capable of incomplete phase retrieval in the presence of noise jumps that exceed 2π/pixel or phase discontinuities that are less than 2π/pixel. However, no $k(\mathbf{r})$ solution of Eq. (1) in this case is unique, because the wrapping operator distorts the statistics of noncorrelated Gaussian noise.

For most applications it is commonly assumed that a wrapped phase exists within the whole image. However, there is another class of images in which

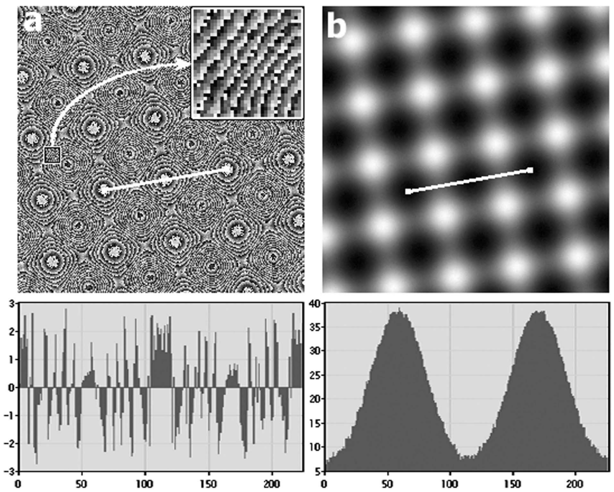

Fig. 2. (a) Example of wrapped phase with a high density of vortices and noise jumps, as shown by the line scan at the bottom. (b) Unwrapped phase map of 512×512 pixels obtained by the solution of Eq. (3). The unwrapped noisy phase, measured in radians and shown below by the same line scan, is pixel to pixel identical to the original noisy phase. Inset in (a), enlarged pixel structure in the boxed area.

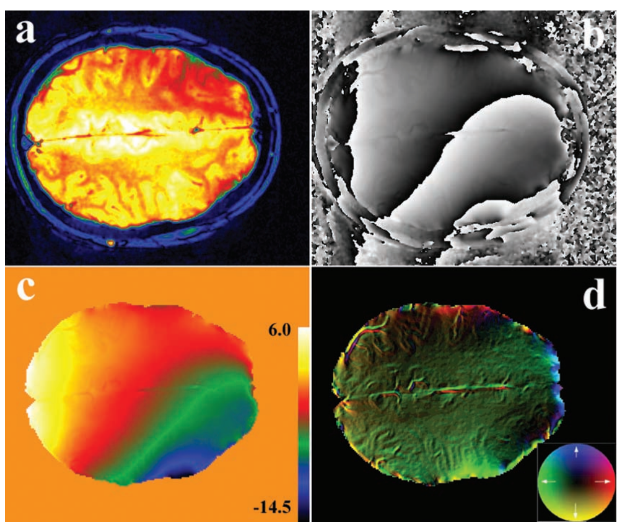

Fig. 3. (a) Amplitude and (b) wrapped phase components of the complex magnetic resonance image recorded with a sampling of 185×210 pixels. Results of the exact solution for (c) an unwrapped phase map and (d) the phase gradients. The temperature color bar in (c) is calibrated in radians. Inset in (d), amplitude and direction of phase gradients in magnetic settings.

the phase exists as a physical quantity in only a bounded area restricted by the imaged object. Let us consider magnetic resonance imaging, which is widely used in medical research (Fig. 3). The complex signal Z of proton magnetic resonance in the two-dimensional case is recorded as $Z = X(x, y) + iY(x, y) = A(x, y)\exp[i\varphi_w(x, y)]$, with the wrapped phase $\varphi_w(x, y)$ defined in only the area of nonvanished amplitude $A(x, y)$. The analysis of an experimental complex image $Z(A, \varphi_w)$ is shown in Fig. 3. Although the amplitude information (Fig. 3a) is widely used in three-dimensional tomography, medical diagnostics, and clinical studies, the applied research based on wrapped phase (Fig. 3b) is hampered by the problem of reliable phase unwrapping. The results in Figs. 3c and 3d show that a new approach with an appropriate object mask solves this problem as well. We get both the quantitative phase map (Fig. 3c) and the phase gradient map (Fig. 3d) related to the distribution of the magnetic field in human brain tissue.

In conclusion, we have presented an exact theoretical solution for the phase-unwrapping problem. Our approach requires only three Fourier transforms with a computing time of $\sim 3N^2 \log N$, where N is the image size in pixels. It provides a deterministic single-step phase unwrapping in the presence of noise and phase vortices in all cases when the problem may have correct physical formulation. For strongly undersampled images (Figs. 1 and 2) it outperforms other advanced algorithms,[13,14] because the minimal theoretically possible kernels for derivatives used in our method are only 2×1 pixels. We believe that the new concept, exact solution, and algorithm will find applications in optics, physics, engineering, and medicine.

This work was supported by the U.S. Department of Energy's Office of Basic Energy Sciences contract DE-AC02-98CH10886. The authors acknowledge T. Ernst and E. Caparelli for recording the raw data used in the analysis of Fig. 3. We would appreciate receiving more data to further test our approach. V. Volkov's e-mail address is volkov@bnl.gov.

References

1. A. V. Oppenheim and R. W. Schafer, *Digital Image Processing* (Prentice-Hall, Englewood Cliffs, N.J., 1975).
2. H. P. Hjalmarson, L. A. Romero, D. C. Ghiglia, E. D. Jones, and C. B. Norris, Phys. Rev. B **32,** 4300 (1985).
3. L. N. Mertz, Appl. Opt. **18,** 611 (1979).
4. G. H. Kaufmann and G. E. Galizzi, Appl. Opt. **41,** 7254 (2002).
5. D. L. Fried, Opt. Commun. **200,** 43 (2001).
6. P. E. Downing, Y. Jiang, M. Shuman, and N. Kanwisher, Science **293,** 2470 (2001).
7. R. Cusack and N. Papadakis, Neuroimage **16,** 754 (2002).
8. V. Pascazio and G. Schirinzi, IEEE Trans. Image Process. **11,** 1478 (2002).
9. E. Volkl, L. F. Allard, and D. C. Joy, eds., *Introduction to Electron Holography* (Plenum, New York, 1999).
10. S. Stramaglia, A. Refice, and L. Guerriero, Physica A **276,** 521 (2000).
11. C. F. Lo, X. Peng, and L. L. Cai, Optik **113,** 439 (2002).
12. P. Soille, Opt. Lasers Eng. **32,** 339 (2000).
13. S. M. Song, S. Napel, N. J. Pelc, and G. H. Glover, IEEE Trans. Image Process. **4,** 667 (1995).
14. M. A. Schofield and Y. Zhu, Microsc. Microanal. Microstruct. **8**(Suppl. 2), 532 CD (2002).
15. V. V. Volkov and Y. Zhu, Phys. Rev. Lett. **91,** 043904 (2003).
16. V. V. Volkov, Y. Zhu, and M. De Graef, Micron **33,** 411 (2002).